

*Venus' Coronae: Impact, Plume, or Other Origin?***Donna M. Jurdy***Department of Geological Sciences, Northwestern University, Evanston, Illinois 60208, USA***Paul R. Stoddard***Department of Geology and Environmental Geosciences, Northern Illinois University, DeKalb, Illinois 60115, USA***ABSTRACT**

Venus' surface hosts hundreds of circular to elongate features, ranging from 60 to 2600 km, and averaging somewhat over 200 km, in diameter. These enigmatic structures have been termed “coronae” and attributed to either tectono-volcanic or impact-related mechanisms. A quantitative analysis of symmetry and topography is applied to coronae and similarly-sized craters to evaluate the hypothesized impact origin of these features. Based on the morphology and global distribution of coronae, as well as crater density within and near coronae, we reject the impact origin for most coronae. The high level of modification of craters within coronae supports their tectonic nature. The relatively young Beta-Atla-Themis region has a high coronal concentration, and within this region individual coronae are closely associated with the chasmata system. Models for coronae as diapirs show evolution through a sequence of stages, starting with uplift, followed by volcanism and development of annuli, and ending with collapse. With the assumption of this model, a classification of coronae is developed based merely on the interior topography. This classification yields corona types corresponding to stages that have a systematic variation of characteristics. We find that younger coronae tend towards being larger, more eccentric, flatter, and generally occur at higher geoid and topography levels than older ones.

## INTRODUCTION

Of the terrestrial planets, Venus most resembles Earth, but with key differences. The two planets have similar size, density and also surface basalt composition; however, Venus undergoes retrograde rotation, has no magnetic field, lacks water, and has a much denser atmosphere. Although Venus does not display Earth-like plate tectonics, it does show evidence of both volcanic and tectonic activity. Here we will argue that numerous, large circular features on Venus, called coronae, are a manifestation of these processes.

Venus' surface hosts nearly 1000 unambiguous impact craters, ranging in diameter from 1.5 to 280 km. The planetary crater density has been used to infer a relatively young surface age for Venus, in the range of 750-300 Ma (Phillips et al., 1992; Schaber et al., 1992). A more recent estimate (McKinnon et al., 1997) widens that range, to 1000-300 Ma. To a first order, the crater distribution approximates a random distribution (Phillips et al., 1992); however, terranes may differ in crater density (Ivanov and Basilevsky, 1993; Price et al., 1996). More specifically, a slight deficit, of about 20 craters, has been documented, statistically, near Venus' chasmata (Stefanick and Jurdy, 1996). The majority of the craters appear pristine in radar images, although slightly less than 200 display clear modification by either volcanic or tectonic activity or both. Craters, when viewed at the highest available resolution, however, often reveal evidence of subtle modification (Herrick, 2006). In addition, some craters show enigmatic, parabolic halos, impact-related phenomena unique to Venus. These parabolic halo-associated craters preserve impact debris that has settled in the presence of zonal winds, and may represent the most recent 10% of Venus' history (Basilevsky and Head, 2002).

Veneras 15 and 16 mapped Venus' surface with radar that Barsukov et al. (1986) used to identify ring-like, uplifted features, named "coronae" or "ovoids." Pronin and Stofan (1990), using corona morphology, further classified 32 features that had been identified on about 20% of the planet, as imaged by Venera radar. With the Magellan probe's improved resolution and radar coverage exceeding 90%, Stofan et al. (1992) were able to catalogue and characterize 362 structures having an "annulus of concentric tectonic features." These coronae and coronae-like features were classified according to morphology; individual features ranged from 60 to 2000+ km in diameter, many of which displayed circular to elliptical annuli and raised interiors.

Coronae on Venus have been attributed to a variety of mechanisms. When coronae were first identified on Venus' surface, they were considered "volcano-tectonic" features because of associated deformation and lava flows (Barsukov et al., 1986). In noting 500 additional circular features of unclear origin, the authors speculated whether these could have resulted from the "reworking" of ancient impact basins (Barsukov et al., 1986). In their analysis of Venera data, however, Pronin and Stofan (1990) selected 21 features for which they identify corona characteristics. From these examples they documented an evolutionary sequence for coronae with initial uplift and volcanism and later annulus development. On the basis of raised topography and associated volcanism, coronae were attributed to diapirs or hotspots, and their clustering and location at tectonic sites further suggested that coronae were related to Venus' global tectonics.

Noting, from Magellan images, the non-random distribution of coronae and the age progression for overlapping coronae, Stofan et al. (1992) attributed coronae to the effects of mantle plumes beneath a stationary venusian surface. Later, Stofan and Smrekar (2005) attributed Venus' large

topographic rises (“regiones”) to mantle plumes. They inferred multiple scales of upwelling on Venus, with coronae operating at an intermediate scale between volcanoes and larger volcanic rises. Furthermore, Stofan and Smrekar (2005) postulated that due to the lack of plate tectonics, Venus may release heat via a larger number of secondary upwellings, coming from a shallower level, which generate plumes. Koch and Manga (1996) replicated the raised rims of coronae with a model for a rising diapir that spreads at the level where it reaches neutral buoyancy. Based on the diapir model, DeLaughter and Jurdy (1999) reclassified coronae according to the extent of interior uplift of each structure, which they interpreted as a measure of stage, or degree of maturity, of individual features. Noting the selective location of coronae, Johnson and Richards (2003) argued that coronae could be due to small-scale transient effects coexisting with larger scale upwellings, such as those that produce major highland provinces. A more complete history and description of the variety of proposed models for coronae formation are provided by Herrick et al. (2005).

Recently, Venus' coronae have once again been interpreted as impact-related. Vita-Finzi et al. (2005) analyzed an expanded database of 514 coronae, of which 362 had been catalogued by Stofan et al. (1992), and the remainder, which they termed "stealth" coronae, were features with incomplete annuli from the catalogue of Tapper et al. (1998). Based on comparison of the morphology and distribution of Venus' coronae with lunar craters, Vita-Finzi et al. (2005) argued that coronae are impact features, and that the variation in corona form results from the location of the impact and subsequent modification. Hamilton (2005) asserted that, on Venus, a gradation exists between pristine, generally accepted craters and much older, highly deformed features, and that circular features classified as coronae are in fact the consequence of ancient impacts. As noted in both these studies, a reinterpretation of coronae as impact features gives a much-

expanded catalogue of craters. Consequently, this would result in a much older estimate of the age of Venus' surface and bring into question the proposed resurfacing event at about 1000-300 Ma. In addition, the identification of Venus' coronae as impact features would require revisiting models for the evolution and heat loss of our sister planet.

In this study, we evaluate a variety of mechanisms that have been proposed to form coronae. Starting with the impact hypothesis, we assess evidence for the age and activity of coronae and compare their distribution with known impact craters. We develop and apply a quantitative approach to compare topographic symmetry of selected, similarly-sized features classified as either coronae or craters. Next, we investigate whether the proposed evolutionary model for coronae results in stages that have systematic characteristics, such as size, shape, and dip. We end with a model for coronae that best explains the observations and note remaining questions.

## **DATASETS**

The Magellan mission, 1990-1994, provided nearly full coverage of Venus. Because of the thick atmosphere, radar was used, operating in three modes: nadir-directed altimetry, Synthetic-Aperture-Radar (SAR) imaging, and thermal emission radiometry. The altimetry footprint was dependent on direction and latitude, but generally ranged between 10 and 30 km, and the vertical resolution was typically 5-50 m. Over its three cycles, the Magellan radar succeeded in imaging 98% of the surface at high resolution (~100 m), changing angle of incidence between cycles (Pettengill et al., 1991, Saunders et al., 1991). Consequently, about 10% of the areas were imaged two or three times with different incident angles, allowing very high resolution topographic analysis using stereo imaging, with optimal lateral resolution exceeding that of the altimetry by a

factor of ~100 (Plaut, 1993). The nearly complete coverage provided by Magellan and Pioneer Venus allowed the gravity field, and corresponding potential field (the geoid), to be determined at a relatively high resolution (order 90) (Sjogren et al., 1997). For our study, we use the geoid field, as well as global altimetry data and the SAR images collected by Magellan.

Classification of coronae remains subjective, as reflected in the numerous published corona catalogues. Herrick et al. (2005), for example, addressed the issue of differentiating volcanoes from coronae, noting the problem that some features are in catalogues of both types. For our analysis we draw our data set from the intersection of the Price and Suppe (1995) and DeLaughter and Jurdy (1999) catalogues (Fig. 1). Price and Suppe (1995) mapped 669 distinct features as coronae, defined as "circular to irregular volcanic-tectonic features characterized by an annulus of concentric deformation," and ranked according to the increasing proportion of "new volcanic flows" associated with each. A set of 335 coronae that DeLaughter and Jurdy (1999) were able to classify derives from their analysis of a total of 394 features from three sources (Stofan et al., 1992, Magee Roberts and Head, 1993, USGS Flagstaff). We further discuss this scheme in a later section.

Impact crater distribution and morphology are the primary tools used to analyze planetary surface ages and processes. We use here the 940-crater catalogue of Phillips and Izenberg (personal communication, 1994; Phillips et al., 1992), as shown in Figure 1. As previously mentioned, these craters have a first-order random global distribution, indicating a near-uniform surface age for Venus. More detailed analysis (Price and Suppe, 1995) suggested a terrane-based density structure, with plains being the most heavily cratered (and thus oldest) terrane. Morphologically, Phillips et al. (1992), using radar imagery, identified the minority of craters that have been

obviously modified: 158 tectonized and 55 embayed, with 19 craters showing clear evidence of being both tectonized and embayed. However, close analysis of craters at very high resolution (<100m), made possible with stereo imaging, reveals tectonic and volcanic activity for numerous craters, suggesting that perhaps most of the craters have been modified (Herrick and Sharpton, 2000; Herrick, 2006). They thus concluded that volcanic activity on Venus may be more widespread than initially believed. It is important to remember, however, that stereo imaging is possible for only a small percentage of the surface, so any such studies are necessarily very limited in their scope. For example, in their study of the Beta-Atla-Themis region, Matias and Jurdy (2005) found only 13 out of 153 craters with the necessary double coverage and only two with triple; thus in that region less than 10% of the craters are candidates for stereo imaging. We use the global crater dataset of Phillips and Izenberg in our analyses, as well as their assessment of modification. We argue that those craters obviously modified, as judged directly from radar images, have suffered alteration to a greater degree than the subtle modifications which can be discerned only with stereo imaging and thus are more indicative of major alteration processes.

Like the Earth, Venus has a global rift system. The 1978 Pioneer missions to Venus provided radar and gravity data that enabled Schaber (1982) to identify a global system of extensional features on Venus, which he cited as evidence of tectonic activity, despite the apparent lack of Earth-style plate tectonics. Schaber attributed the extension to upwelling-related processes, such as at Earth's continental rift zones, but noted the global scope of these extension zones, similar in scale to Earth's mid-ocean ridge system. These rift zones can be fit by four great circle arcs (Schaber, 1982). Using the nearly global coverage provided by Magellan, Solomon et al. (1992) characterized these rift zones, termed "chasmata," as rugged regions with some of Venus' deepest troughs, extending 1000s of kilometers. They noted the extreme relief, with elevation changing

as much as 7 km in just 30 km distance. The 54,464 km-long Venus chasmata system, as defined in greater detail by Magellan, can be fit by great circle arcs at the 89.6% level, and when corrected for the smaller size of the planet, the total length of the chasmata system measures (Jurdy and Stefanick, 1999) within 2.7% of the 59,200 km length of the spreading ridges determined for Earth by Parsons (1981). The chasmata with the greatest relief on Venus experienced linear rifting during the latest stage of tectonic deformation (Head and Basilevsky, 1998). The chasmata shown in Figure 1 were derived from mapping by Price and Suppe (1995). The geoid of Venus, as determined from Magellan data, is superposed on the other features in Figure 1. We display a smooth geoid field (orders 10-30), similar in scale to the features of interest.

Venus' regiones, broad areas of relief, number about 10. Stofan and Smrekar (2005) noted that regiones range in diameter from 1000 to 2700 km and rise between 0.5 and 2.5 km above the surrounding terranes, and have positive gravity anomalies. A regio might be dominated by rifts, such as Atla and Beta discussed here (Fig. 2), or by volcanism, like Imdr, Bell and Dionne, or be dominated by coronae, as Themis (Stofan and Smrekar, 2005). The rift-dominated regiones, Atla and Beta, have the greatest topographic expression. Atla and Beta are the sites of several rift intersections and the two major geoid highs on Venus. Curiously, the geoid "bulls' eyes" also coincide with the intersections of arcs fitting the chasmata. The current deformation of Venus' surface has been described as being caused by a swell-push force, the result of a steep gradient of the geoid height (Sandwell et al., 1997). Thus, these areas may be experiencing the most intense deformation on the planet, and the network of rifts may have formed in response to this deformation.

Coronae occur in many rift segments, yet none actually occurs at these intersection points. Perhaps just as remarkable, Atla has a partial ring of four domal coronae, all between 4 and 5 geoid contours from the crest, while Beta has a partial ring of 6 or so calderic coronae between three and four contours from its crest. Possibly, thicker crust at the regiones inhibits the formation of coronae in association with chasmata (Bleamaster and Hansen, 2004). On the other hand, using geoid-topography ratios, models for these highlands suggest thinning of a thick lithosphere (150-350 km) to as little as 100 km over an anomalously hot (by as much as 400-1000K) asthenosphere (Moore and Schubert, 1997). Such an analysis (which requires wavelengths greater than 600 km) is not appropriate for coronae, unfortunately, given their smaller size, as well as their close proximity to each other. This distribution of coronae led Stoddard and Jurdy (2003) to hypothesize that Atla represents a younger phase of large-scale upwelling than Beta (Fig. 3). Craters, initially formed flat, show some tilting around Atla and Beta (Stoddard and Jurdy, 2003; Jurdy et al., 2003) consistent with an active uplift of Atla and a recent slumping of Beta. Additionally, coronae often intertwine with chasmata or are contained by the chasmata walls (Fig. 4).

## **TESTING THE IMPACT ORIGIN HYPOTHESIS**

An ancient impact origin for coronae - as opposed to recent endogenic activity - makes several testable predictions. If, as suggested by Hamilton (2005, 2007) and Vita-Finzi et al. (2005), coronae are ancient impact features, with ages of up to 3.9 Ga, they should be significantly more heavily cratered than the younger, average-aged surface. Previously, Namiki and Solomon (1994) evaluated impact crater density within coronae interiors, finding evidence for significantly lower densities within late-stage coronae, which they defined as being dominated by volcanism. Price

and Suppe (1995) evaluated crater density on various terranes, and found that coronae, as a terrane type, have low crater densities. Using the corona dataset of Stofan et al. (1992), DeLaughter and Jurdy (1997) found low crater density out to four corona radii near the uplifted coronae, whereas the density was about normal for those coronae with collapsed interiors. In our analysis, we find that although the 669 coronae from the map of Price and Suppe (1995) occupy 10.6% of Venus' surface, they host only 7.0% (66 of 939) of the crater population (Table 1), suggesting that the coronae are, as a whole, younger than the average surface age. On the other hand, an excess (again, when compared to surface area) of Phillips and Isenberg's (1992) unambiguously tectonized craters (24, or 15.2%, of 158 total) are found within coronae, indicating that coronae are more tectonically active than the average surface region. Somewhat surprisingly, embayed craters are under-represented within coronae (5.5% of the planetary population on 10.6% of the planet's surface). Of course, with smaller populations, interpretations from these statistics become less certain. For a random distribution, the standard deviation is the square root of the number counted (Fisher, sect. 15, 1973). Thus for a count of 4 items, one standard deviation would include counts of 2 to 6 ( $4 \pm 2$ ). Obviously for such small sets, it would not be possible to achieve counts that deviate enough from the average to achieve two full standard deviations.

Another consequence of the impact origin hypothesis is that coronae, as ancient impact sites, should be concentrated on the oldest areas of the planet's surface. However, we claim the opposite is true – that coronae are actually concentrated in the youngest region of Venus' surface. Coronae are most heavily concentrated in the so-called "BAT" region - the area between Atla, Beta, and Themis regiones (Fig. 2). We define this region roughly as between 45°N and 45°S, 180°E and 315°E. Using these boundaries, we find that 292 (43.6%) of all coronae lie within the

BAT region, which itself comprises only 26.4% of the planet's surface. Unambiguous BAT region impact craters total 224 (23.9%), but if instead we were to assume that coronae are additional impact sites, then 32% of all impact features are found here, which would then indicate a somewhat older than average surface age. However, by most accounts the BAT region represents the youngest, most active region on Venus (e.g. Head and Basilevsky, 1998).

Several lines of evidence support this claim. Examining the set of young, commonly agreed-upon craters shows the BAT region to be somewhat deficient, arguing for a younger, not older region. Also, the BAT region contains nearly two thirds (by area) of all rifts as identified by Price and Suppe (1995). In their global sequence of tectonic deformation, Head and Basilevsky (1998) find that linear rifting prevailed in the latest stage of events. That rifts are among the most active (or most recently active) features on Venus can be further demonstrated by the relative dearth of craters and plethora of tectonized and embayed craters (Table 1). Crater Uvaysi (2.3°N, 198.2°E) provides additional support of our conclusion that the BAT region has experienced very recent activity. This crater, at the intersection of three chasmata and nearly at Atla Regio's crest, has been classified as both tectonized and embayed. Opportunely, the clear evidence of modification is coupled with the presence of a radar-dark parabola with Uvaysi, near the apex of Atla Regio. As argued by Matias and Jurdy (2005), these two occurrences constrain the volcanism and tectonism of the crater to be recent, because parabolic haloes remain from only the last 10% of Venus' surface history. Uvaysi is one of eleven of the planet's 19 craters that are both tectonized and embayed, nearly 60%, contained within the BAT region; more than double what would be expected based solely on area. Looking at cratering and stratigraphy, Vezolainen et al. (2004) suggested that Beta uplift began after the average age of the surface ( $T$ ), and has continued until after  $0.5 T$ . Basilevsky and Head (2007), based on stratigraphic relations to neighboring terranes,

also suggested recent or current uplift of Beta Regio. Taken in its entirety, the BAT region itself also shows the relative lack of craters and excess of modified craters seen by the rifts.

Furthermore, the two largest geoid highs coincident with Atla and Beta regiones may indicate a dynamic nature of these features, and thus additional support for a young age for the BAT region.

Coronae, if indeed ancient impacts, should predate active rifts. Coronae and chasmata, however, are intimately related as can be seen in Figure 2. Even a cursory inspection of Hecate and Parga chasmata (extending between Atla and Beta, and Atla and Themis, respectively) depicted in Figures 2 and 4 shows this relation. In many cases, corona boundaries seem constrained by the rift walls (Fig. 4). A more quantitative analysis of corona and rift orientation was also undertaken. This comparison shows that while there is no apparent relation for coronae outside rifts; coronae within rifts tend to parallel the rift axis (Fig. 5). Given their locations and orientations, we find that coronae within rifts must develop as part of the rifting process and/or continue forming post-rifting. If, on the other hand, coronae were ancient, predating the rifts, then we would find them not in the rifts, but bisected by the rifts. On the basis of the above analyses, we here conclude that coronae cannot be ancient impacts.

Any model for impact history needs to address the lack of cratering between these two eras (ancient corona impacts and young crater impacts), and the lack of transitional features between coronae and craters. In positing an old "impact age" for coronae, neither Vita-Finzi et al. (2005) nor Hamilton (2005) addressed in detail transitional craters, i.e., those younger than ancient "corona" impacts but older than the more commonly accepted impact set. The size distributions of craters and coronae (Vita-Finzi et al., 2005; their Fig. 6) clearly show two well-defined and distinct populations.

Spatial distribution has been proposed as a means for determining the origin of coronae. Vita-Finzi et al. (2005), in their argument for an impact origin for coronae, claimed that the corona distribution on Venus resembles global impact distributions on both Venus and the Moon. We challenge their conclusion on two grounds. First, we assert that the lunar comparison is flawed, as the utilized catalogue of 1562 lunar craters, while the best currently available, consists of named features only, and thus has a strong near-side bias, as well as a bias against high-latitude features (personal communication, Deborah Lee Soltesz, USGS, 2006). Correspondingly, their lunar "crater density traces," based on that catalogue, peak at 0°N, 0°E (Vita-Finzi et al., 2005, their Fig. 10). Second, we observe that the venusian crater distributions were incorrectly displayed by Vita-Finzi et al. (2005). When corrected for decreasing area with latitude, the venusian distribution appears random in both latitude (with the exception of the drop-off towards the south pole, due to gaps in satellite coverage) and longitude, unlike the corona distribution (Fig. 6). We therefore argue that the corona distribution on Venus differs significantly from the crater distribution and cannot be used to argue for similar origins. Furthermore, we attribute the complementary distribution of craters and coronae with longitude to crater removal by corona-related volcano-tectonic activity.

### *Quantitative analysis of circular symmetry*

Craters by their nature are circular. They are excavated by a roughly hemispherical shock wave, and thus almost regardless of impact angle, will be round rim-and-basin structures (Melosh, 1989). Underlying structural features, such as faults, and later tectonic deformation can modify crater shape. Perhaps, therefore, the strongest test of an impact origin for coronae is the circularity of these features. .

Here we introduce an approach for the assessment of a feature's circular symmetry. Using altimetry data we compare, by cross-correlation, multiple profiles across a single feature. Jurdy and Stoddard (2005, <http://jove.geol.niu.edu/faculty/stoddard/05ChapmanPoster.pdf>), provide an example in which Mead crater and two coronae, all measuring about 280 km across, were analyzed. They found that for each corona, profiles cross-correlated at only 25-30% of perfect cross-correlation. Profiles for Mead crater, however, correlated at a much higher level, 80%. Here, we perform an expanded study, for five features generally classified as craters, and six whose classification as coronae has been questioned by Hamilton (2007, this volume), the results of which are summarized in Figure 7. We choose only the largest craters, since altimetry data are too coarse to allow enough data points for analyses of smaller features, and also because they are of similar size to the coronae in our study. For each feature, 36 profiles (taken every ten degrees) are extracted from the altimetry data. The average slope is removed from each profile (to nullify the effects of any post-emplacement tilting), and the results are aligned and then averaged together. For each feature, each profile was then correlated against the average, and the correlations themselves were averaged to give an assessment of circular symmetry. A perfectly circular feature would have a correlation average of 100% - indicating that each profile was identical to the average profile.

Figures 7(a-e) show the results for five craters. Note that for Mead, Cleopatra, Meitner, and Isabella the profiles display the typical rim and basin structure expected for craters, but for Klenova (e) the average profile is more domal, with only a few of the individual profiles looking crater-like. The “contested” coronae are shown in Figures 7(f-k). The average profiles for Eurynome (f), Maya (h), and C21 (i) appear crater-like, albeit with more variation among the

individual profiles than seen in the generally agreed-upon craters. Anquet (g) has a rim-and-basin structure, but unlike typical craters, the basin is elevated above the surrounding plains. Acrea (k) appears to be a small hill in a large depression, again with a high degree of variation. Ninhursag (j) is clearly domal, and cannot be viewed as a crater.

The variability of the profiles, and thus the circularity of each feature, is summarized in Figure 7(l). Those features universally agreed upon as craters (in yellow) have the highest correlation percentages – all at or above 80%, with the exception of Klenova. The disputed features (Figures 7f-k) are not as circular, although C21 is close. Based on this analysis, we conclude that Klenova has been mischaracterized as an impact crater, and also that C21, a feature previously classified as corona may indeed be of impact origin (Table 2). The cases for Maya and Eurynome are more ambiguous. We propose that this type of correlation analysis can be used in an objective assessment of circularity, and therefore the origin, of the remaining catalogue of similar features.

To address the non-circularity of coronae, Vita-Finzi et al. (2005) and Hamilton (2007) suggested deformation of these features by post-impact tectonic activity. Such activity must be local rather than regional; otherwise a preferred orientation of the long axes of coronae, reflecting the tectonic stress regime, should be apparent. This is not the case, either in relation to the major tectonic features or to the chasmata (Fig. 5). We have found no correlation between the long axis of individual coronae and their dip direction, as might be expected if corona were initially circular and their ellipticity and orientation were both related to later deformation.

## EVOLUTIONARY MODEL

Here we consider an evolutionary model for coronae based on rising diapirs, as an alternative to the impact hypothesis. Coronae were assigned to three distinct morphological groups using Magellan altimetry (DeLaughter and Jurdy, 1999). In this classification, *domal* coronae (numbering 54) are distinguished by a central uplift with no surrounding moat, and may have associated radial fracturing, often only visible in the SAR images. A flattened interior and an annular moat characterize 93 *circular* coronae; portions of their interiors may be lower than the surrounding plains. *Calderic* coronae, with more than 50% of the interior lower than the surrounding plains, constitute the majority (188) of DeLaughter and Jurdy's (1999) classified features, and display raised rims and annular moats. The three groups are gradational; consequently, boundaries in this classification are arbitrary. In Figure 8, we show the classification along with radar images of representative coronae corresponding to the stages. The attraction of this scheme is the simplicity of application: one only needs to establish the elevation of the corona interior relative to its surroundings. A further appeal of the approach is the possibility that the three groups may represent evolutionary stages of corona development, from initial diapir uplift to ultimate collapse.

For our analysis of classified coronae, we use the subset of DeLaughter and Jurdy's (1999) catalogue that corresponds to those 669 distinct features mapped by Price and Suppe (1995) as coronae. A total 287 were matched to the morphologically classified coronae (DeLaughter and Jurdy, 1999). This correlation yielded a smaller set: 39 domal coronae, 83 circular, and 165 calderic, with 382 features remaining unclassified. A more sophisticated scheme could be devised to incorporate more features, but in our study we use this subset.

Next, we investigate the consequences of this classification scheme: Do the three groups of coronae - domal, circular and calderic - represent stages of corona evolution? If so, then an age progression should be evident from the density of impact craters and their modification. As noted, the distribution of impact craters on Venus very nearly approaches random. In Table 1, the crater counts are documented for all coronae, as well as the morphological subgroups. Some intriguing patterns emerge. Coronae cover 10% of the surface of Venus, but only contain 7% of the craters – indicating a younger than average age. Likewise, although domal coronae occupy 0.9% of the total surface area, they contain only 0.3% of the craters, and thus crater density on these coronae is about 1/3 of what would be expected for average-aged features, and is also less than that for all coronae as a group. Additionally, the circular and calderic coronae have only 3/4 of the number of craters expected for their areas. These crater densities are consistent with the inferred stages, i.e., with the domal being the youngest. The circular and calderic coronae, however, have an overpopulation, by 50%, of tectonically modified craters. This analysis (Table 1) shows that coronae, as a set, stand out as younger features, ones with lower crater density. Similarly, Price and Suppe (1995), in their terrane-based study, found that coronae and corona-like features are second only to large volcanoes in having the lowest crater density. Furthermore, our study provides evidence of tectonic modification, as would be expected for the proposed older coronae. In addition, crater densities and modification are consistent with the classification of coronae by evolutionary stage. Alternatively, if coronae were of ancient impact origin, we would expect to find them more heavily cratered, not less, than the average terrane.

***Do coronae evolve in size, shape and orientation through their lifetime?***

If these coronae do, in fact, represent a diapir life cycle, then we would expect to see systematic variations in some coronal attributes, such as size, shape, dip, topographic and geoidal elevations, etc., independent of the morphological criteria by which the coronae were classified. Figure 9a shows length versus dip, and Figure 9b shows the eccentricity versus dip for all coronae, comparing the whole set. The geoid versus topography is shown in Figure 9c. The domal coronae are shown as yellow, circular as green and calderic as blue, with the remaining unclassified ones as black. Although the data show considerable scatter, analysis reveals some interesting patterns.

Quartile analysis provides a useful characterization of the range of values for a set. In quartile analysis the values range from  $q_0$  to  $q_4$ . The lowest fourth of the values range from  $q_0$  to  $q_1$ , the next fourth of the values range from  $q_1$  to  $q_2$ , similarly the third quarter range from  $q_2$  to  $q_3$ , and the final, top quarter range from  $q_3$  to  $q_4$ . The numbers  $q_1$  and  $q_3$  are often referred to as the first and third quartiles, and  $q_2$  is usually referred to as the median. The numbers  $q_0$  and  $q_4$  are the minimum and maximum values. For a set with a statistically-defined “normal distribution,” the quartiles can be related to the standard deviation: for a normal (or Gaussian) distribution, 68.3% of the values lie within one standard deviation of the mean. Alternatively, the range between the first and third quartiles contains 50% of the values and the points are within 0.675 standard deviations of the mean (Fisher, 1973). We apply this simple, yet informative analysis to the sets of coronae.

The quartile analysis documents a distinct separation by stage (Table 3). Size strongly depends on the stage: 3/4 of the domal coronae are larger than 3/4 of the calderic ones, with circular

coronae intermediate in size. Why are domal (yellow) bigger and more eccentric? Perhaps the initial corona eruption corresponds to an active diapir that later withdraws. The ellipticity is also a function of stage: more than half the circular and calderic coronae have eccentricities less than 0.50 while more than half the domal ones have eccentricities over 0.70. A tilt was determined for each feature by determining the dip of a best fitting plane through the region. The tilt or dip determined for coronae also seems related to the stage: 3/4 of the domal dip less than 3/4 of the calderic, and circular are intermediate. Although a continuum exists between coronae stages, some characteristics distinguish uplifted coronae from largely collapsed ones: the domal coronae are larger, more eccentric, but flatter than the calderic coronae. Systematically, the circular coronae lie between the domal and calderic for almost all parameters we defined. These patterns further support the morphologic classification of coronae (DeLaughter and Jurdy, 1999) as a simply-determined, but useful, indication of stage or degree of maturity of individual features. Thus, the consistent continuum implies an evolutionary sequence, and we infer that the morphology of coronae indicates the stage with the domal being youngest, circular intermediate and calderic as the oldest. On the basis of these observations, we suggest that an objectively-defined algorithm could be universally applied to the entire catalogue, allowing classification of many, if not most, of these features.

## **DISCUSSION**

In our study we have examined the cratering record, distribution, and morphology of coronae. We argued that these preclude an impact origin for these features. A tectono-volcanic origin better fits our observations. We then presented and evaluated a model that considers coronae as manifestations of diapir evolution.

### ***What mechanism formed Venus' coronae?***

Crater density inside and near coronae argues for their being young and therefore volcanically and tectonically active features. Impact crater density within coronae lies below the planetary average; yet even with this lower density, the proportion of obviously tectonized craters considerably exceeds the number expected based on the total coronal area. Also, coronal distribution is more consistent with a volcano-tectonic than with an impact origin. Coronae are strongly concentrated in the young BAT region and are closely associated with rifts, themselves sites of recent, if not ongoing, activity. We also show that longitudinal corona distribution, a pulse centered in the BAT region, clearly differs from the more random arrangement of impact craters. Even if we were to assume all coronae are impact features, the combined corona and crater distribution is still not random in longitude (Figure 6). Taken together, these observations are more consistent with coronae being young, active features, rather than being ancient impact sites.

### ***Are coronae Venusian analogs of Earth's plumes?***

Although there are hundreds of features that have been identified as coronae, only 54 of these have more than 50% of their interiors raised above the exterior (here classified as domal and potentially active). These correspond to 0.9% of the surface of the planet. Are these plumes on Venus? Here, we define a "plume" as a deep-seated, long-lived thermal perturbation with a volcanic and tectonic surface expression. On Earth, the combination of plume and plate tectonic activity leads to Hawaiian-style island chains. On Mars, where no large-scale lateral tectonic activity is believed present, plume activity remains localized, resulting in the largest known shield volcanoes, such as Olympus Mons. On Venus, if coronae are in fact caused by plumes, there could be as many as 50. In comparison, Earth's currently active plumes have been variously

numbered from a mere handful to well over 100. No unanimity exists on a catalogue of hotspots for Earth. For example, two analyses that correlated hotspot locations with geoid highs to infer the dynamic link (Chase, 1979; Crough and Jurdy, 1980) employed 24 and 42 hotspots respectively. So, comparing to these analyses, if all 54 domal coronae were active plumes this would correspond to Venus' having an excess of 30% to more than 100% when compared with its sister planet, Earth. This number, though high, may not be unreasonable for a planet lacking plate tectonics to transport heat from the interior. Nonetheless, the presence of over 600 coronae, implying that number of plumes in the last 1000-350 Ma of Venus, does seem inordinately high, and therefore argues against a distinct plume source for each of these. We agree with Stofan and Smrekar (2005) that the regiones, such as Atla, Beta, Themis, and Phoebe, would correspond better to planetary plumes, i.e., large-scale uplifts. The smaller number of regiones (~10), as discussed earlier, agrees more with our understanding about the capability of a planet's core to generate plumes that support uplifts. Ideally, the size and strength of individual plumes should be considered in this comparison, but these characteristics exceed the scope of this paper.

The areal pattern of the domal coronae presents another argument against their having deep sources: in Figure 2, for example, note the four closely-spaced domal coronae (yellow) between two contour lines around Atla's peak. Active plumes beneath each of these locations do not seem reasonable. In the terrestrial studies cited, hotspots are generally restricted to positive "residual" geoid regions, once the dominating effect of subduction has been removed. However, on Venus, coronae are found to correlate with mid-geoid levels (Jurdy and Stefanick, 1999). This effect is apparent in Figure 9c, as almost a topographic limit, beyond which the domal coronae - the ones we infer as active - cannot exceed.

Shallow diapirs may offer a more reasonable explanation for coronae. Admittance studies of several coronae (Hoogenboom et al., 2004) showed coronae as active upwellings, which has been interpreted to indicate isostatic compensation (Stofan and Smrekar, 2005). Based on fluid dynamic models, Hansen (2003) argued that coronae could be attributed to compositional diapirs, as opposed to the large rises and regiones, like Atla and Beta, for which thermal plumes are often invoked. We find that the observations presented in this paper are consistent with a model of coronae as diapirs, either thermal or compositional, evolving through a sequence of stages, starting with uplift, followed by volcanism and development of annuli, and ending with collapse. As we have shown, a classification of coronae based merely on the interior topography leads to stages with a systematic set of characteristics. Younger coronae are larger, more eccentric, flatter, and generally occur at higher geoid and topography levels.

A fuller understanding of coronae, and therefore of their underlying causes, could be achieved by extending the approaches we have taken to the entire set of 669 features mapped as "coronae" by Price and Suppe (1995). The study we presented in this paper was more limited in scope and applied to the subset of coronae that had been categorized by DeLaughter and Jurdy (1999) by inspection. Any classification by visual examination is open to interpretation, thus we propose utilizing an objective algorithm to assign each feature to a class based on its topography - whether uplifted, flat or collapsed. The characteristics of each feature, such as tilt, size, ellipticity, altitude, geoid, and particularly the circularity can then be determined quantitatively as we demonstrated here. We suspect that the group of coronae showing collapsed interiors may harbor a few impact craters, such as C21, as described in our analysis here. A complete and systematic examination of all features on Venus classified as coronae should allow further evaluation of the diapir versus impact models for origin of these enigmatic circular features.

The relationships among coronae, regiones, and chasmata are complex, but in all likelihood hold the key to understanding the resurfacing processes for Venus, and in turn, the global heat dissipation mechanisms. In the absence of Earth-like plate tectonics, plumes, whether on the scale of regiones or coronae, must play an important role in both phenomena.

## **ACKNOWLEDGMENTS**

We thank Alexander Basilevsky, Claudio Vita-Finzi and Gillian Foulger for their careful and thoughtful reviews. Warren Hamilton's comments on the first version of this paper helped us in developing an approach to assess circularity of features. We thank Michael Stefanick for his assistance with statistics and interpretation of data.

**REFERENCES CITED**

Barsukov, V. L., plus 29 others, 1986, The geology and geomorphology of the Venus surface as revealed by the radar images obtained by Venera 15 and 16: *Journal of Geophysical Research*, v. 91, D378-398.

Basilevsky, A. T., and Head, J. W., 2002, Venus: Timing and rates of geologic activity: *Geology*, v. 30, p. 1015-1018.

Basilevsky, A. T., and Head, J. W., 2007, Beta Regio, Venus: Evidence for uplift, rifting and volcanism due to a mantle plume, in *GSA Special Paper, Plumes, Plates, and Planetary Processes*. ed. G. R. Foulger and D. M. Jurdy, this volume, in press.

Bleamaster, L. F, and Hansen, V. L., 2004, Effects of crustal heterogeneity on the morphology of chasmata, Venus: *Journal of Geophysical Research*, v. 109(E0), 2004, doi: 10.1029/2003JE002193.

Chase, C. G., 1979, Subduction, the geoid, and lower mantle convection: *Nature*, v. 282, p. 464-468.

Crough, S. T., and Jurdy, D. M., 1980, Subducted lithosphere, hotspots, and the geoid: *Earth and Planetary Science Letters*, v. 48, p. 15-22.

DeLaughter, J. E., and Jurdy, D. M., 1997, Venus resurfacing by coronae: Implications from impact craters: *Geophysical Research Letters*, v. 24, p. 815-818.

DeLaughter, J. E., and Jurdy, D. M., 1999, Corona classification by evolutionary stage: *Icarus*, v. 139, p. 81-92.

Fisher, R. A., 1973, *Statistical methods for research workers*: New York, Hafner, 362 pages.

Hamilton, W. B., 2005, Plumeless Venus preserves an ancient impact-accretionary surface, *in* *Plates, Plumes, and Paradigms*, Geological Society of America Special Paper 388, Foulger, G. R., Natland, J. H., Presnall, D. C., and Anderson, D. L., eds., p. 781-814.

Hamilton, W. B., 2007, An alternative Venus, in *GSA Special Paper, Plumes, Plates, and Planetary Processes*. ed. G. R. Foulger and D. M. Jurdy, this volume, in press.

Hansen, V. L., 2003, Venus diapirs: Thermal or compositional?: *Geological Society of America Bulletin*, v. 115, p. 1040-1052.

Head, J. W., and Basilevsky, A. T., 1998, Sequence of tectonic deformation in the history of Venus: Evidence from global stratigraphic relationships: *Geology*, v. 26, p. 35-38.

Herrick, R. R., 2006, Updates regarding the resurfacing of Venusian impact craters: *LPSC XXXVII* (abstract).

Herrick, R. R., and Sharpton, V. L., 2000, Implications from stereo-derived topography of Venusian impact craters: *Journal of Geophysical Research*, v. 105 (E8),

Herrick, R. R., Dufek, J., and McGovern, P. J., 2005, Evolution of large shield volcanoes on Venus: *Journal of Geophysical Research*, v. 110, doi: 10.1029/2004JE002283.

Hoogenboom, T., Smrekar, S. E., Anderson, F. S., and Houseman, G., 2004, Admittance survey of type 1 coronae on Venus: *Journal of Geophysical Research*, v. 109, doi: 10.1029/2003JE002171.

Ivanov, M. A., and Basilevsky, A. T., 1993, Density and morphology of impact craters on tessera terrain, *Venus GRL*, v. 20, p. 2579-2582.

Johnson, C. L., and Richards, M. A., 2003, A conceptual model for the relationship between coronae and large-scale mantle dynamics on Venus: *Journal of Geophysical Research*, v. 108(E6), 5058, doi: 10.1029/2002JE001962.

Jurdy, D. M., and Stefanick, M., 1999, Correlation of Venus surface features and geoid: *Icarus*, v. 139, p. 93-99.

Jurdy, D. M., and Stoddard, P. R., 2005, Uplift and Rifting on Venus: Role of Plumes [abs]: AGU Chapman Conference: "The Great Plume Debate." .

Jurdy, D. M., Stoddard, P. R., and Matias, A., 2003, Upwellings on Venus: Evidence from Coronae and Craters [abs.]: GSA Penrose Conference: "Plume IV: Beyond the Plume Hypothesis."

Koch, D. M., and Manga, M., 1996, Neutrally buoyant diapirs: A model for Venus coronae:

Geophysical Research Letters, v. 23, p. 225-228.

Magee Roberts, K., and Head, J. W., 1993, Large-scale volcanism associated with coronae on

Venus: Implications for formation and evolution: Geophysical Research Letters, v. 20, p.

1111-1114.

Matias, A., and Jurdy, D. M., 2005, Impact craters as indicators of tectonic and volcanic activity

in the Beta-Atla-Themis region, Venus, *in* Plates, Plumes, and Paradigms, Geological

Society of America Special Paper 388, Foulger, G. R., Natland, J. H., Presnall, D. C., and

Anderson, D. L., eds., p. 825-839.

Matias, A., Jurdy, D. M., and Stoddard, P. R., 2004, Stereo Imaging of Impact Craters in the Beta-

Atla-Themis (BAT) region, Venus, 35th Lunar and Planetary Science, Houston, Texas,

Abstract #1383.

Melosh, H. J., 1989, Impact cratering: New York, Oxford University Press.

Moore, W. B. and Schubert, G., 1997, Venusian crustal and lithospheric properties from nonlinear

regressions of highland geoid and topography: *Icarus*, v. 128, p. 415-428.

Namiki, N., and Solomon, S. C., 1994, Impact crater densities on volcanoes and coronae on

Venus: Implications for volcanic resurfacing: *Science*, v. 265, p. 929-933.

Parsons, B., 1981, The rates of plate creation and consumption: *Geophysical Journal of the Royal astronomical Society*, v. 67, p. 437-448.

Pettengill, G.H., Ford, P.G., Johnson, W.T.K., Raney, R.K., and Soderblom, A., 1991, Magellan: Radar performance and data products: *Science*, v.252, p.260-265.

Phillips, R. J., Raubertas, R. F., Arvidson, R. E., Sarkar, I. C., Herrick, R. R., Izenberg, N., and Grimm, R. E., 1992, Impact craters and Venus resurfacing history: *Journal of Geophysical Research*, v. 97, p. 15923-15948.

Plaut, J.J., 1993, Stereo Imaging, in *Guide to Magellan Image Interpretation: JPL Publication 93-24*, California Institute of Technology, Pasadena, California, p.33-43.

Price, M., and Suppe, J., 1995, Constraints on the resurfacing history of Venus from the hypsometry and distribution of tectonism, volcanism, and impact craters: *Earth, Moon, and Planets*, v. 71, p. 99-145.

Price, M. H., Watson, G., Suppe, J., and Brankman, C., 1996, Dating volcanism and rifting on Venus using impact crater densities: *Journal of Geophysical Research*, v. 101, p. 4657-4671.

Pronin, A. A., and Stofan, E. R., 1990, Coronae on Venus: Morphology, classification, and distribution: *Icarus*, v. 87, p. 452-474.

- Sandwell, D. T., Johnson, C. L., Bilotti, F., and Suppe, J., 1997, Driving forces for limited tectonics on Venus: *Icarus*, v. 129, p. 232-244.
- Saunders, R.S. and G.H. Pettengill, 1991, Magellan: Mission summary, *Science*, v.252, p.247-249.
- Schaber, G. G., 1982, Venus: Limited extension and volcanism along zones of lithospheric weakness: *Geophysical Research Letters*, v. 9, p. 499-502.
- Schaber, G. G., Strom, R. G., Moore, H. J., Soderblom, L. A., Kirk, R. L., Chadwick, D. J., Dawson, D. D., Gaddis, L. R., Boyce, J. M., and Russell, J., 1992, Geology and distribution of impact craters on Venus: What are they telling us?: *Journal of Geophysical Research*, v. 97, p. 13257-13301.
- Sjogren, W.L., Banerdt, W.R., Chodas, P.W., Konopliv, A.S., Balmino, G., Barriot, P., Arkani-Hamed, J., Colvin, T.R., and Davies, M.E., 1997, The Venus gravity field and other geodetic parameters, in *Venus II, Geology, Geophysics, Atmosphere, and Solar Wind Environment*, ed. S.W.Bougher, D.M. Hunten and R.J. Phillips, pages 1125-1161.
- Solomon, S. C., Smrekar, S. E., Bindschadler, D. L., Grimm, R. E., Kaula, W. M., McGill, G. E., Phillips, R. J., Saunders, R. S., Schubert, G., Squyres, S. W., and Stofan, E. R., 1992, Venus tectonics: An overview of Magellan observations: *Journal of Geophysical Research*, v. 97, p. 13199-13255.

- Stefanick, M., and Jurdy, D. M., 1996, Venus coronae, craters and chasmata: *Journal of Geophysical Research*, v. 101, p. 4637-4643.
- Stoddard, P. R., and Jurdy, D. M., 2003, Uplift of Venus Geoid Highs: Timing from Coronae and Craters: 34th Lunar and Planetary Science, Houston, Texas, Abstract #2129.
- Stoddard, P. R. and Jurdy, D. M., 2004, Venus' Atla and Beta Regions: Formation of chasmata and coronae [abs.]: EOS, Transactions of the American Geophysical Union.
- Stofan, E. R., Sharpton, V. L., Schubert, G., Baer, G., Bindschadler, D. L., Janes, D. M., and Squyres, S. W., 1992, Global distribution and characteristics of coronae and related features on Venus: Implications for origin and relation to mantle processes: *Journal of Geophysical Research*, v. 97, p. 13347-13378.
- Stofan, E. R., and Smrekar, S. E., 2005, Large topographic rises, coronae, large flow fields, and large volcanoes on Venus: Evidence for mantle plumes?, *in* Plates, Plumes, and Paradigms, Geological Society of America Special Paper 388, Foulger, G. R., Natland, J. H., Presnall, D. C., and Anderson, D. L., eds., p. 841-861.
- Tapper, S. W., Stofan, E. R., and Guest, J. E., 1998, Preliminary analysis of an expanded corona database: 29th Lunar and Planetary Science, Houston, Texas, Abstract #1104.

Vezolainen, V., Solomatay, V. S., Basilevsky, A. T., and Head, J. W., 2004, Uplift of Beta Regio: Three-dimensional models: *Journal of Geophysical Research*, v. 109, do.i:10.1029/2004E002259.

Vita-Finzi, C., Howarth, R. J., Tapper, S. W., and Robinson, C. A., 2005, Venusian craters, size distribution, and the origin of craters, *in* *Plates, Plumes, and Paradigms*, Geological Society of America Special Paper 388, Foulger, G. R., Natland, J. H., Presnall, D. C., and Anderson, D. L., eds., p. 815-823.

## FIGURE AND TABLE CAPTIONS

Figure 1. Eckert IV (equal area) projection of Venus' surface, centered on 120°W, showing craters (red dots), chasmata (pink regions), coronae (gray, yellow, green, blue regions, as defined in the text) and geoid (order 10) 30 m contours. Unshaded area represents region depicted in Figure 2.

Figure 2. Beta-Atla-Themis regiones (BAT) region. Pink: Chasmata. Yellow: Domal coronae. Green: Circular coronae. Blue: Calderic coronae (classifications from DeLaughter and Jurdy, 1999). Dark gray: Unclassified coronae. Open circles: Pristine craters. Red upward-pointing triangles: Embayed craters. Light blue downward-pointing triangles: Tectonized craters. Purple circles: Craters that have been both tectonized and embayed. Craters with dark halos are indicated by black arcs. Contour lines are for geoid order 10, 30m contours. Unshaded area is shown in detail in Figure 4.

Figure 3. Model for evolution of regio features, such as Atla and Beta.

Figure 4. Detail of Parga chasm exemplifying the intertwining relationship between many coronae (yellow, green, blue, green, and gray) and chasmata (pink). Region is from 240°E to 270°E, 0°S to 25°S. 5° grid. Radar image is from [http://planetarynames.wr.usgs.gov/images/v40\\_comp.pdf](http://planetarynames.wr.usgs.gov/images/v40_comp.pdf).

Figure 5. Corona orientation relative to rifts. Orientation of the long axis of the best-fitting ellipse to each corona is compared to the orientation of the nearest rift segment. a.) For coronae within the central rift graben, there is a preferred corona orientation parallel to sub-parallel the rift axis. b.) Corona near, but not in, rifts do not show this behavior. Color scheme (yellow, green, blue) matches classification scheme of DeLaughter and Jurdy (1999).

Figure 6. Coronae (red, solid lines), crater (blue, dashed lines), and combined (purple, solid lines) densities with latitude, longitude for Venus ( $10^\circ$  bins). Lighter background indicates BAT region limits.

Figure 7. Comparison of topographic profiles across craters and coronae on Venus. For each of Figures (a) through (k), thirty six individual profiles are shown, in blue through green, based on orientation of the profile. Blue is W-E, proceeding clockwise through S-N, E-W, N-S, and back to W-E. The average profile is depicted by the bold red line. (a-e) Profiles for 5 craters. (f-k) Profiles for 6 coronae. (l) Summary of circularity study for these 11 features, based on the average correlation among the individual profiles. A 100% average correlation would indicate 36 identical profiles, and perfect circular symmetry. Features (a-e), commonly accepted as craters, are depicted in yellow, green indicates features (f-k), features commonly accepted as coronae.

Figure 8. Coronae classification scheme, with example profiles. A: Domal corona Selu, centered at  $42.5^\circ\text{S}$ ,  $6^\circ\text{E}$ , diameter = 150 km. B: Domal/Circular transitional corona Earhart,  $71^\circ\text{N}$ ,  $136^\circ\text{E}$ , 185.5 km. C: Circular corona Kuan-Yin,  $4.3^\circ\text{S}$ ,  $10^\circ\text{E}$ , 125 km. D: Circular/Calderic transitional corona Demeter,  $55^\circ\text{N}$ ,  $295^\circ\text{E}$ , 333.5 km. E: Calderic corona Holde,  $53.5^\circ\text{N}$ ,  $155^\circ\text{E}$ , 100 km.

Profiles after DeLaughter and Jurdy (1999). Radar images for Selu, Kuan-Yin, and Holde from <http://planetarynames.wr.usgs.gov/vgrid.html>.

Figure 9. Comparison of various coronal parameters, by corona classification. Yellow - domal coronae. Green - circular coronae. Blue - calderic coronae. Black - unclassified coronae.

(a) Length vs. dip for coronae (b) Eccentricity vs. dip for coronae (c) Topography vs. geoid, cross-hairs indicate average values and standard deviations for each set.

Table 1 - Crater density in coronae, rifts, and the BAT region. Number - total number of each feature on Venus' surface. % of area - Total percentage of Venus' surface area covered by each type of feature. For crater columns, the total number of craters found on each type of feature is given, as well as the percentage of the total number of that type of crater found on Venus. For example, there were 24 tectonized craters found on all coronae, which represents 15.2% of the 158 tectonized craters found on Venus.

Table 2- Location, size, circularity (as measured by correlation percentage), commonly-accepted classifications, and suggested new classifications for craters larger than 100 km in diameter and selected coronae.

Table 3 - Quartiles for coronae characteristics. Eccentricity, length and dip given for each corona type with median (q2) and top (q3) and bottom (q1) quartiles.

TABLE 1

	Number of features	Coverage (% of Venus' surface area)	<u>Craters on feature type</u>		<u>Tectonized craters on feature type</u>		<u>Embayed craters on feature type</u>		<u>Tec &amp; Emb craters on feature type</u>	
			#	% of total craters	#	% of tectonized craters	#	% of embayed craters	#	% of T & E craters
<b>All Coronae</b>	669	10.6	66	7.0	24	15.2	3	5.5	2	10.5
<b>Domal (Y)</b>	39	0.9	3	0.3	1	0.6	0	0.0	0	0.0
<b>Circular (G)</b>	83	2.0	14	1.5	5	3.2	1	1.8	1	5.3
<b>Calderic (B)</b>	164	2.2	15	1.6	5	3.2	0	0.0	0	0.0
<b>Rift segments</b>	57	8.3	59	6.3	32	20.3	8	14.5	7	36.8
<b>Bat Region</b>	1	26.5	224	23.9	44	27.8	27	49.1	11	57.9

**TABLE 2**

<b>Feature</b>	<b>Latitude (°N)</b>	<b>Longitude (°E)</b>	<b>Diameter (km)</b>	<b>Correlation %</b>	<b>Common Classification</b>	<b>New Classification</b>
Joliet-Curie	-1.7	62.4	100.9	81	Crater	Crater
Bonheur	9.7	288.8	102.2	84	Crater	Crater
Cleopatra	65.9	7	105	86	Crater	Crater
Stanton	-23.2	199.3	107	88	Crater	Crater
Meitner	-55.5	321.7	140	94	Crater	Crater
Klenova	78.2	104.7	141.9	43	Crater	Corona? (Domal)
Isabella	-29.2	204.2	176	93	Crater	Crater
Mead	12.5	57	268.7	80	Crater	Crater
Ninhursag	-38	23.5	113	64	Corona	Corona (Domal)
C21	29	243	200	74	Corona	Crater
Maya	23	98	225	63	Corona	Crater?
Eurynome	26.5	94.5	200	34	Corona	Corona? (Circ)
Anquet	26.5	98	225	53	Corona	Corona (Circ)
Acrea	24	243.5	250	47	Corona	Corona (Cald)

**TABLE 3****Eccentricity**

	q1	q2	q3
Domal (Y)	.505	.700	.735
Circular (G)	.410	.490	.610
Calderic (B)	.410	.510	.640

**Length (km)**

	q1	q2	q3
Domal (Y)	142	188	281
Circular (G)	129	167	225
Calderic (B)	75	102	150

**Dip (degrees)**

	q1	q2	q3
Domal (Y)	.051	.062	.082
Circular (G)	.057	.101	.169
Calderic (B)	.086	.128	.219

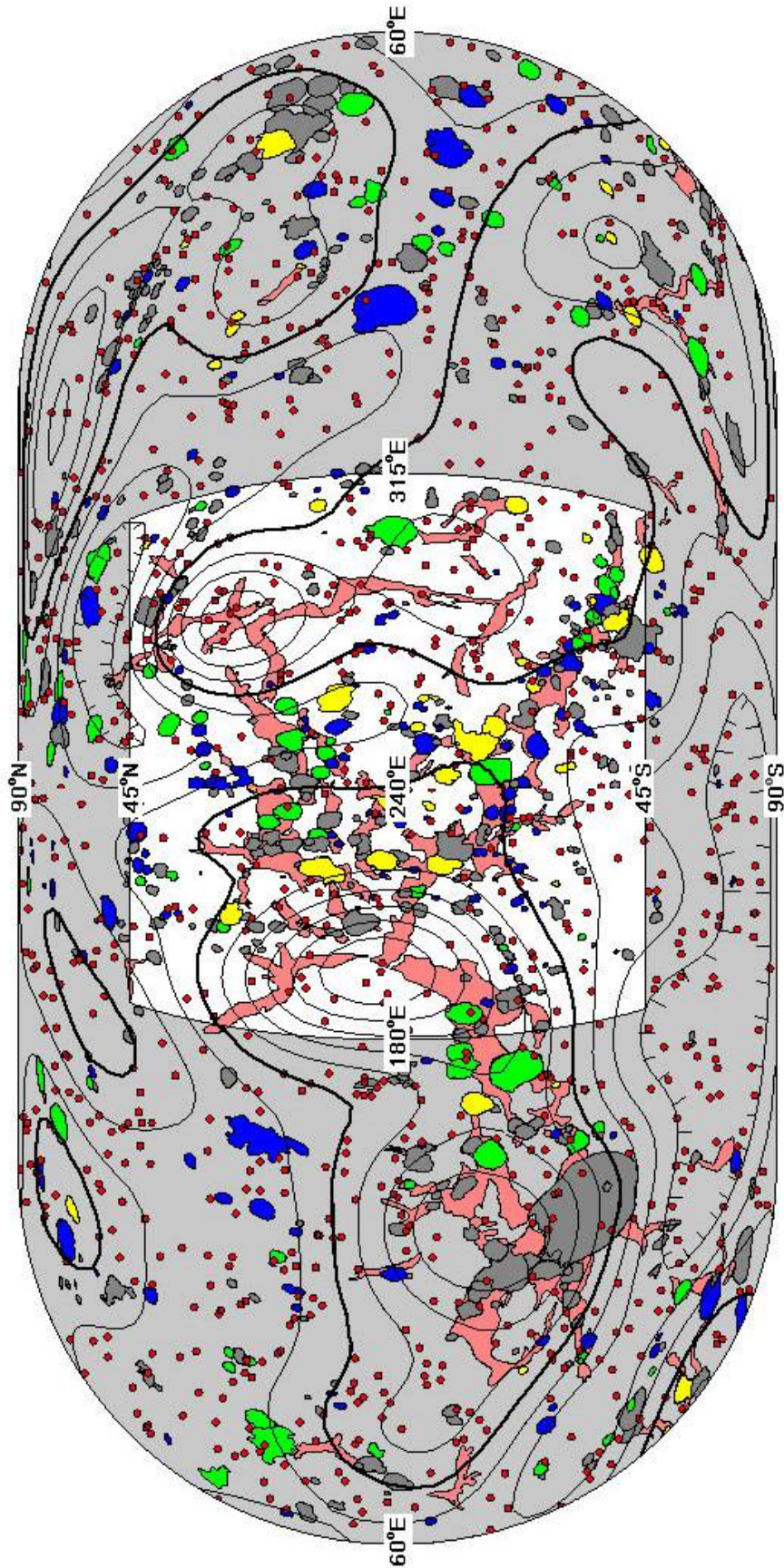


Figure 1

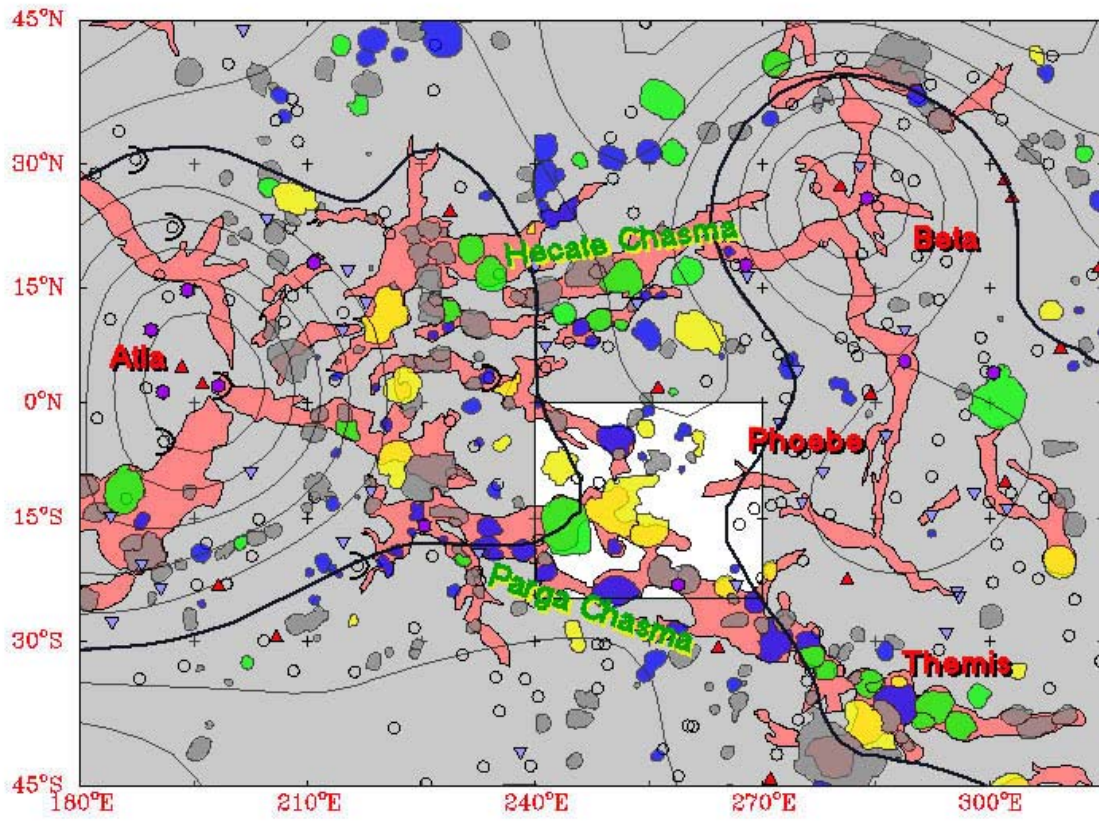


Figure 2

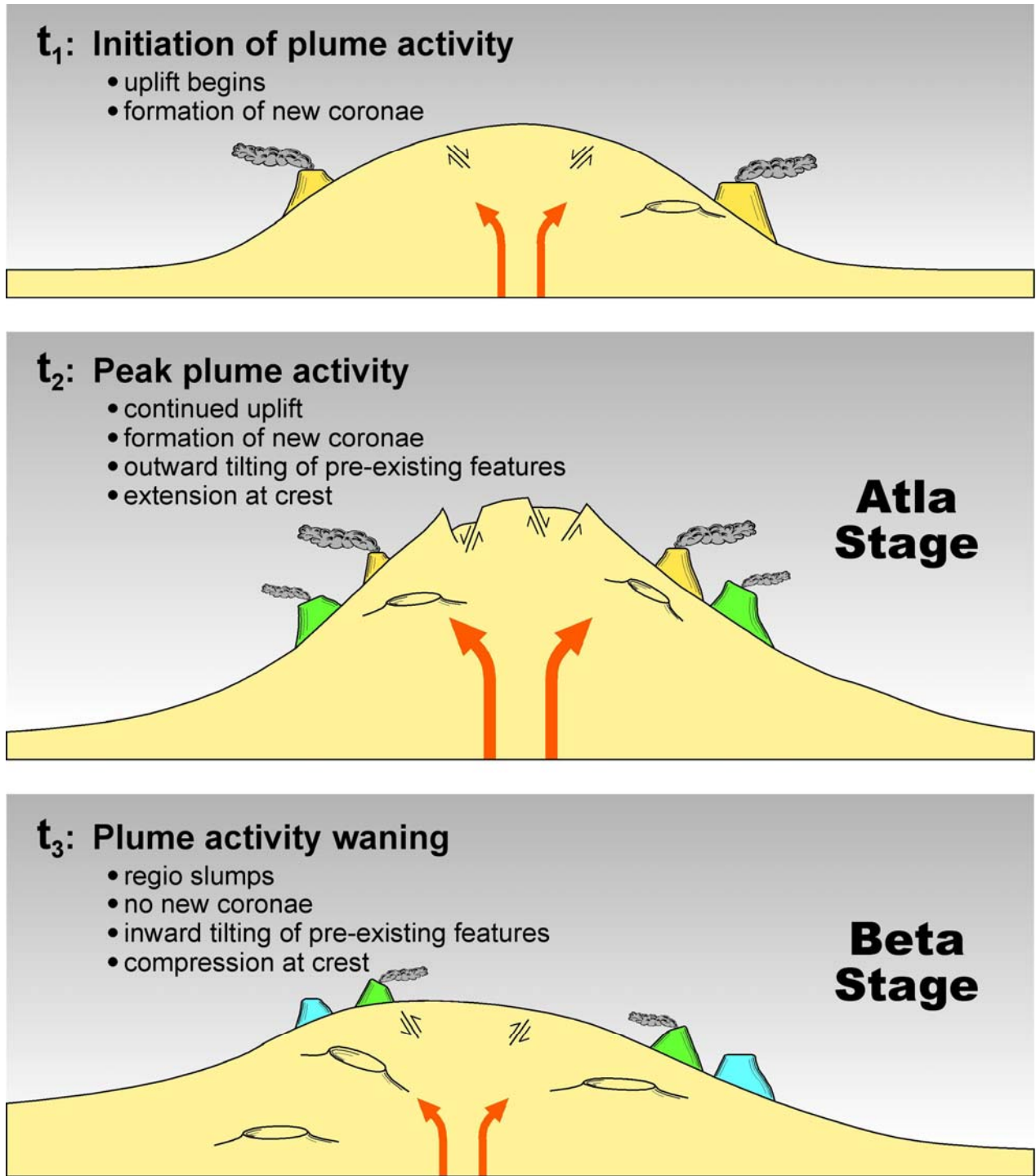


Figure 3.



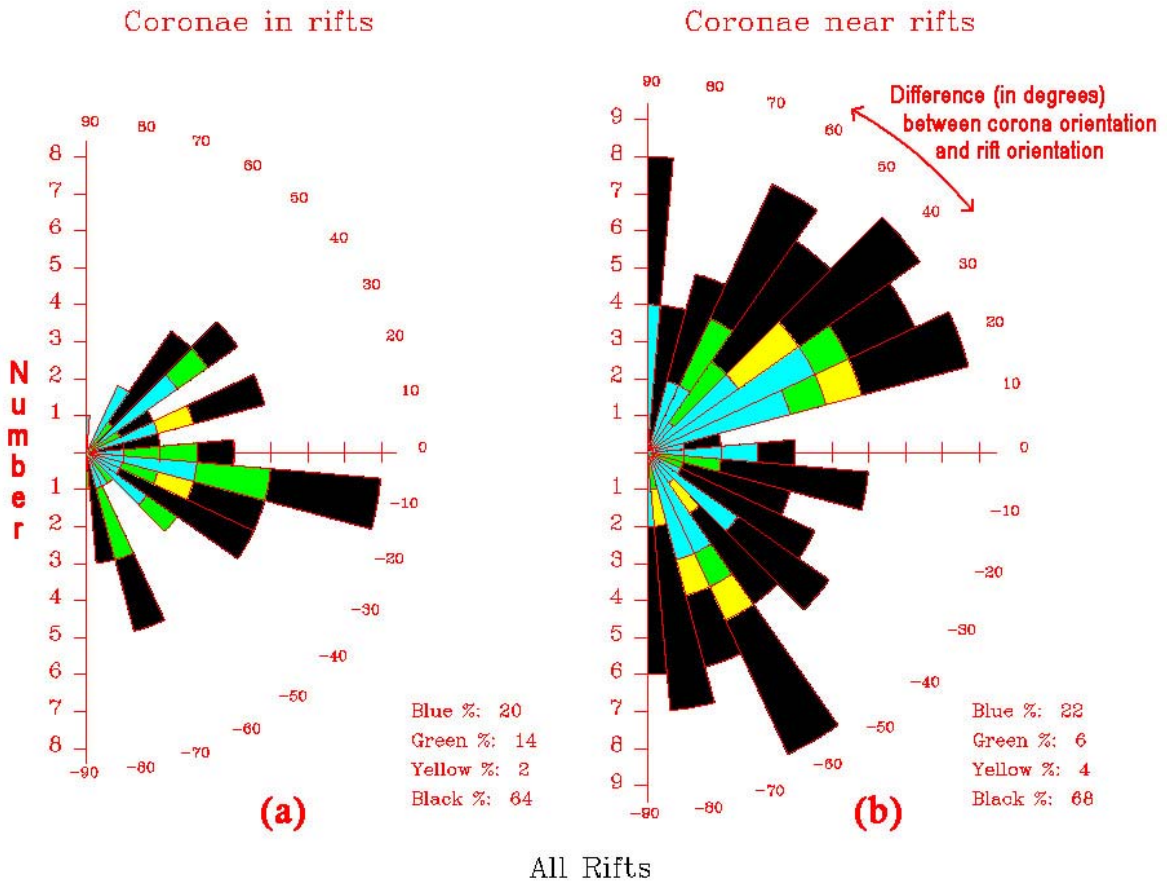


Figure 5.

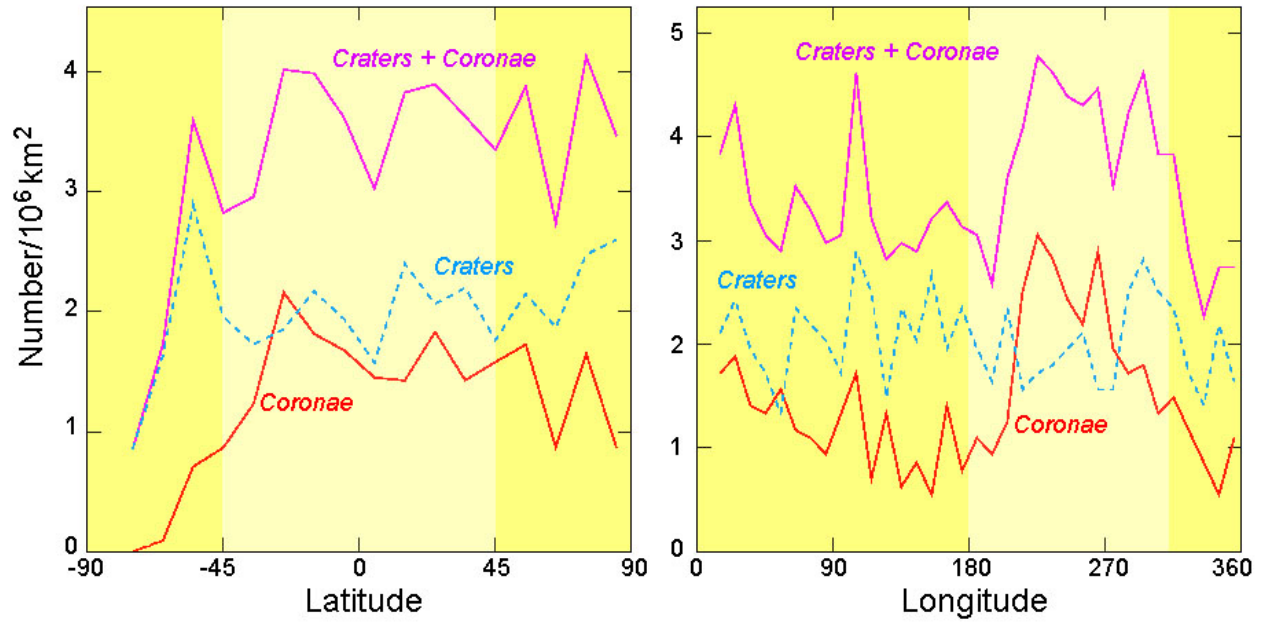


Figure 6.

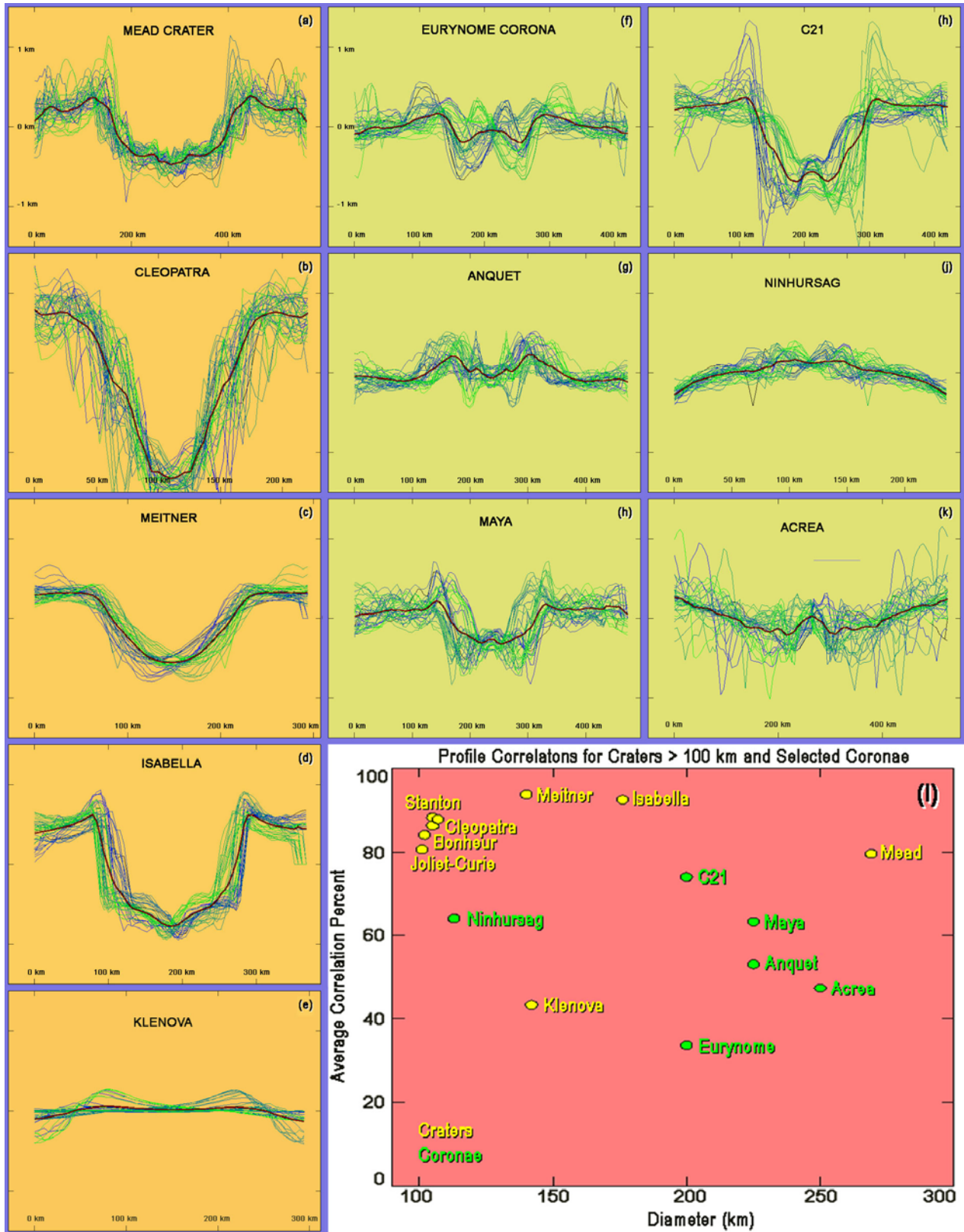


Figure 7.

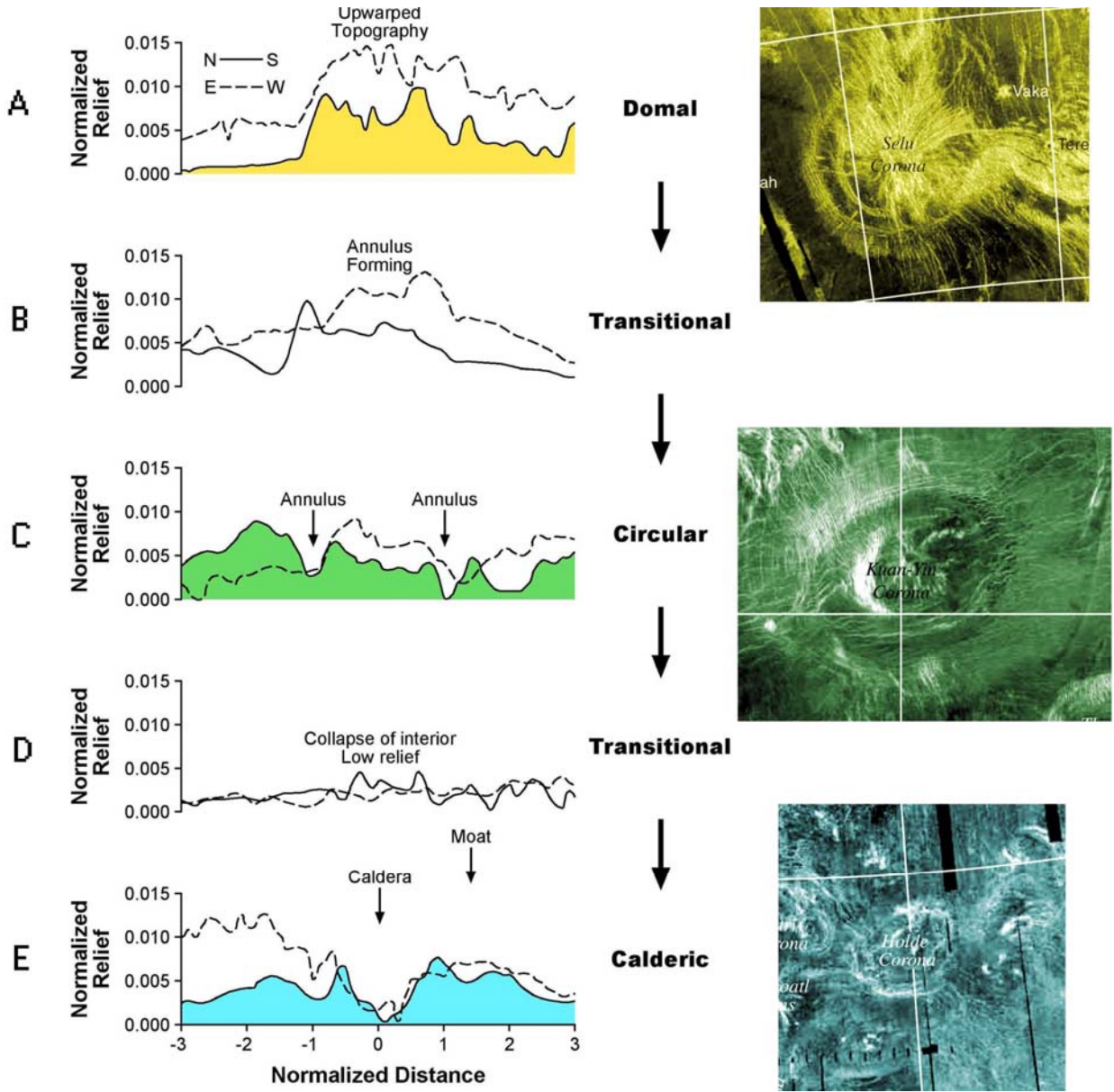


Figure 8.

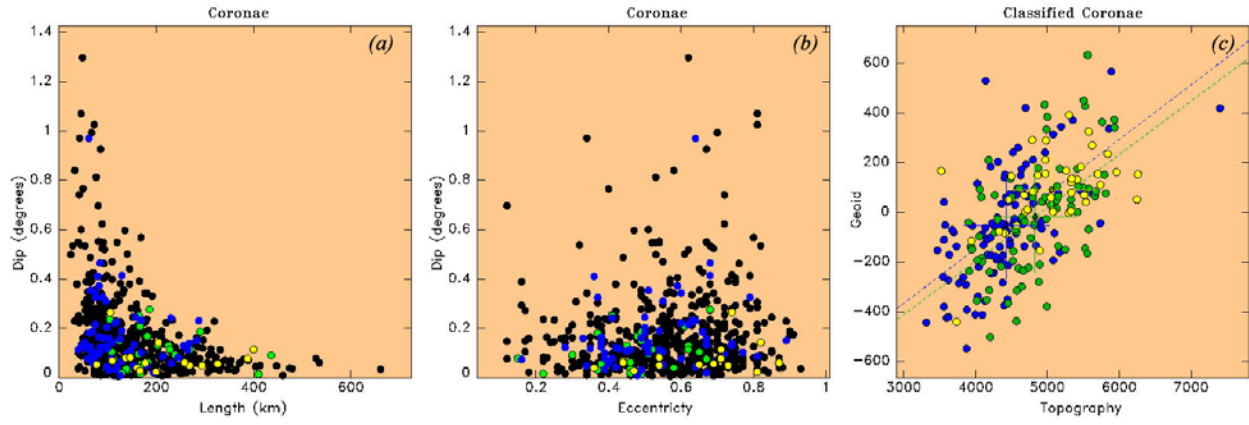


Figure 9.